

# Application of Vortex Induced Vibration Energy Generation Technologies to the Offshore Oil and Gas Platform: The Feasibility Study

T. Yui Khing, M. A. Zahari, S. S. Dol

**Abstract**—Ocean current is always available around the surrounding of SHELL Sabah Water Platform and data are collected every 10 minutes, 24 hours a day, for a period of 365 days. Due to low current speed, conventional hydrokinetic power generation is not feasible, thus leading to the study of low current enabled vortex induced vibration power generation application. In this case, the design of a vortex induced vibration application is studied to obtain an optimum design for the VIV oscillator. Power output is then determined to study the feasibility of the VIV application in low current condition.

**Keywords**—Renewable energy, Vortex induced vibration, Turbulence, Lock-in.

## I. INTRODUCTION

CURRENTLY renewable energy such as wind energy, solar energy and ocean energy are highly focused in the feasibility test of replacing conventional fuels to operate an offshore oil and gas platform. Some of the offshore platforms have already started to exploit a renewable energy sources to generate power supply to lessen consumption of fuels. For example, a new offshore platform in the Southern North Sea is operated by using power generated from renewable energy sources which are wind and solar energy [1]. Unfortunately, the production of electricity from these renewable sources can be unpredictable and inconsistent as wind and solar energy often rely on the weather and climates condition [2]. In addition, an environmental impact of wind power on wildlife is generating concern. As the rotating blade of wind turbine is usually positioned high up in the air, they are known to kill birds that fly over it especially on migratory birds [3]. Due to the fact that these forms of energy are unreliable, new form of alternative energy needs to be studied for offshore application. Ocean energy, which is known as world's largest storage of renewable energy seems like an ideal alternative source of energy due to their availability around the offshore platform [3]. Electricity can be generated by converting the kinetic energy of the ocean's current flow through a hydroelectric power generation. However, not all of the ocean's energy technology exist currently is suitable due to the ocean low current speed. For instance, current turbine energy is unable to generate energy when the current speed is too slow to spin the blade on turbine. Wave Energy Project in 1996 reported that

energy extraction based on tides and currents turbines can only work for current flow stronger than 2 m/s [4]. Thus, newer technology needs to be developed to make power generation not only renewable, but also can generate energy from low current flow. One viable solution that meets these criteria is a hydroelectric power extraction system based on Vortex Induced Vibration (VIV). VIV-based system works by constraining a cylinder horizontally in the water with single degree of freedom, causing the cylinder to be able to move in upward and downward motion as fluid passes through it [5]. When comparison is being done between VIV application and conventional hydrokinetic application, VIV is rather superior due to the fact that most of the other hydrokinetic systems require the current flow to be greater than 2 m/s, and only able to give an output within a small range of frequencies of oscillating wave. VIV on the other hand are able to operate even with very slow current speed, depending on the size of the application designed. There is no alteration or posing of any environmental changes towards the ocean or disrupting the water traffic in the ocean.

Based on previous study, VIV-powered system has an ability to generate power in the range of current speed of 0.26 to 2.6 m/s [6]. VIV-powered systems seem a great idea in generating alternative energy for offshore application as it is not only renewable but also environmental friendly.

This paper aims to investigate an optimum design for the VIV oscillator in order to generate power for offshore platform. The targeted platform for this study is SHELL Malaysia Oil and Gas Sabah Water Platform, with the rated power consumption is approximately 10 MW. Based on the data collected from the targeted platform, the rated power output is determined in order to meet the demand of power consumption of this platform.

## II. LITERATURE REVIEW

### A. Vortex Induced Vibration

Vortex-Induced Vibration (VIV) is turbulence motion induced on bluff body that generates periodic irregularities lift forces on the body and resulting oscillating movement perpendicular to fluid flow as shown in Fig. 1 [6]. Normally, the present of VIV is being avoided by many structures dealing with the fluid flow in order to reduce the fatigue caused by it. However in terms of power generation, the idea of enhancing such phenomenon is brought into handy in order to maximise the extraction of energy from fluid.

M. A. Azizi and S. S. Dol are with the Department of Mechanical Engineering, Curtin University, Miri, Sarawak, Malaysia (e-mail: muhd.azizi@curtin.edu.my, sharulsham@curtin.edu.my).

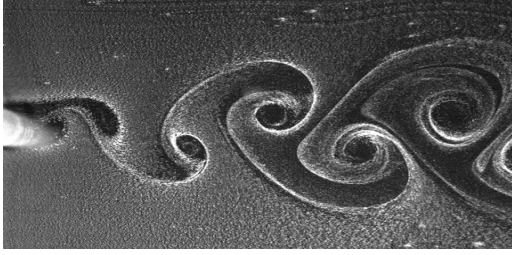


Fig. 1 Vortex shedding periodic pattern

### B. Reynolds Number

Basically, the behaviour of Vortex Street depends on the range of Reynolds number,  $Re$  of flow. The range of  $Re$  targeted in this research are in the range of  $300 < Re < 3 \times 10^5$  which is known as “Fully Turbulent Vortex Street” regime for the natural low-flow [6].  $Re$  can be determined using (1), where  $U$  is the flow velocity,  $D$  is the cylinder diameter and  $\nu$  is the kinematic viscosity of fluid.

$$Re = UD/\nu \quad (1)$$

### C. Strouhal Number

Non-dimensional parameter that describes the vortex shedding frequency to the oscillating flow mechanism is known as Strouhal Number,  $St$  as shown in (2), where  $f_s$  is vortex shedding frequency:

$$St = (f_s D)/U \quad (2)$$

Fig. 2 shows that  $St$  is almost 0.2 for smooth surfaces within the range of  $300 < Re < 10^5$ , which matches well to the fully developed turbulent vortex street. Thus, Strouhal number 0.2 will be used as a constant value in this research [7]. Then, shedding frequency can be calculated as (3):

$$f_s = (St \times U)/D \quad (3)$$

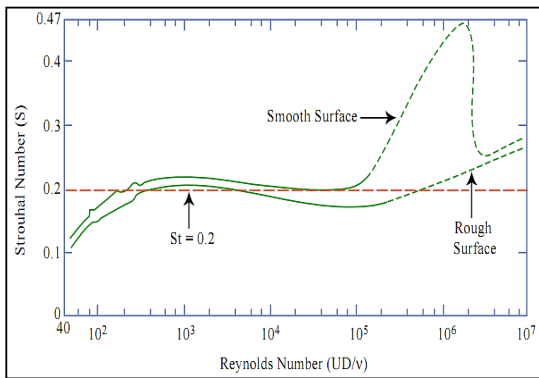


Fig. 2 Strouhal Number vs. Reynolds Number [7]

### D. Lock-in Phenomenon

The main reason as in why VIV application is able to work far better than other conventional hydroelectric generator-based application is due to the presence of “Lock-in” phenomenon. Lock-in phenomenon is a condition when vortex

shedding frequency becomes close to the natural frequency of the body. It is one of the unique aspects for high output of VIV application as large amplitudes of forced vibration is being produced. In this study, the variation of spring constant is carried out to observe how lock-in affects the power output of a VIV. It is essential to find the range of shedding frequency that matches with the natural frequency,  $f_n$  to design energy harnessing device. The natural frequency of the body can be calculated using (4), where  $k$  is spring stiffness and  $m_{app}$  is mass applied to the cylinder.

$$f_n = (1/2\pi) (\sqrt{k/m_{app}}) \quad (4)$$

For the total mass of application needs to be calculated for further calculation of natural frequency, the following cylinder properties were determined as:

$$M_{pipe} = \rho_{cyl} \times L + M_{add} \quad (5)$$

$$Volume = (\pi/4) \times D^2 \times L \quad (6)$$

$$M_{dis} = \rho_{water} \times Volume \quad (7)$$

The material considered in constructing the oscillator in this research is Magnesium Alloy M10600 due to its high corrosion resistance and high tensile strength properties [8]. This alloy is having the density of  $1800 \text{ kg/m}^3$ .

$$M_{app} = M_{pipe} + M_{dis} \quad (8)$$

By matching the natural frequency with shedding frequency for lock in condition [ $f_s = f_n$ ], spring stiffness,  $k$  value is calculated by (3):

$$k = [f_s \times 2\pi]^2 \times M_{app} \quad (9)$$

### E. Lift Force of Cylinder

The oscillator is consisting of smooth cylindrical cylinder. Based on previous studies available on the lift coefficient experienced by smooth cylindrical cylinder, the lift coefficient experienced by the oscillator is approximately 0.6 [9]. With the lift coefficient kept constant, the lift force can be calculated using (10):

$$F_L = 0.5 \rho_{fluid} U^3 DLC_L \quad (10)$$

where  $D$  is the diameter of the cylinder,  $L$  is the length of cylinder,  $C_L$  is the lift coefficient experienced by the cylindrical oscillator,  $\rho_{fluid}$  is the density of sea water, and  $U$  is the speed of current flow.

### F. Maximum Amplitude of Cylinder

The amplitude of the cylinder oscillates can be determined based on (11)

$$y(t) = \frac{F_L \sin(\omega_n t + \frac{\pi}{2})}{k \sqrt{\left(1 - \left(\frac{f_s}{f_n}\right)^2\right)^2 + 4\zeta^2 \left(\frac{f_s}{f_n}\right)^2}} \quad (11)$$

This equation is demonstrating how the cylinder amplitude is responding with respect to the diameter of the cylinder, as well as with respect to time. Based on numerous background research done on oscillating a smooth cylinder, the damping,  $\zeta$  is assumed to be 0.06 [9]. With the availability of this equation, amplitude of the oscillating cylinder can be determined.

*G. Y-velocity of Cylinder*

After determining the amplitude of the oscillating cylinder, the Y-velocity of the cylinder can then be calculated by differentiating the amplitude equation with respect to time as shown in (12) and (13):

$$v(t) = \frac{d}{dt} y(t) \quad (12)$$

$$v(t) = \frac{F_L \omega_n \cos(\omega_n t + \frac{\pi}{2})}{k \sqrt{\left(1 - \left(\frac{f_s}{f_n}\right)^2\right)^2 + 4\zeta^2 \left(\frac{f_s}{f_n}\right)^2}} \quad (13)$$

The Y-velocity varies with the amplitude of the oscillating cylinder. The determination of Y-velocity as well as the amplitude of the oscillating cylinder is important to identify the frequency of lock-in of the cylinder.

*H. Power Output of Cylinder*

In order to find out the approximate power output of cylinder oscillator, mathematical modelling is used in this research. The energy stored within the system in total is subjected to the potential energy of the spring, as well as the kinetic energy gained by the system which is shown in (14):

$$E = (0.5kx^2) + (0.5mv^2) \quad (14)$$

Based on (14),  $x$  can be substituted with amplitude  $A$  in order to describe clearer in the application of VIV oscillator. When amplitude  $A$  is at its maximum, the velocity  $v$  on the other hand will be zero, simplifying the equation into as (15):

$$E = 0.5 kA^2 \quad (15)$$

On the other hand, the RMS power output of a VIV application is based on the oscillator's mechanical energy, the potential energy of the spring connecting the oscillator to the frame of the system, as well as the kinetic energy of the moving oscillator. This correlation can be expressed as (16).

$$P = E = kx\dot{x} + m\dot{x}\ddot{x} \quad (16)$$

where  $\dot{x}$  is the change of position with respect to time of the oscillator, and  $\ddot{x}$  is the acceleration determined from the velocity term. The mathematical equation used to determine the maximum power  $P_{max}$  can be simplified into (17):

$$P(t) = v(t) \cdot F_L \cdot \sin(\omega_n t) \quad (17)$$

The maximum power determined can then be used to determine the RMS power output of the system using (18):

$$P_{rms} = P_{max}/\sqrt{2} \quad (18)$$

III. CURRENT SPEED DATA COLLECTION

With the collected data from SHELL Malaysia, the average monthly current speed hitting around the platform 50 m below sea level are plotted as shown in Fig. 3.

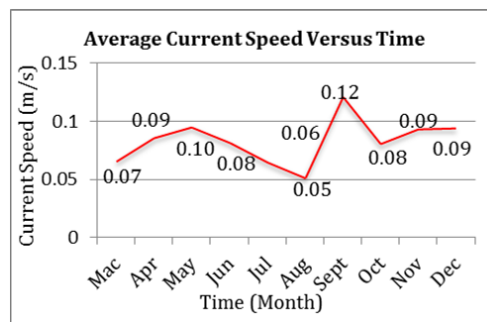


Fig. 3 Average current speed collected on Shell Sabah Water Platform in 2008

Based on collected data, the lowest average current speed of the month was in August, with the average speed of only 0.05 m/s, while the highest average current speed was in September, with speed achieving as high as 0.12 m/s. With such low current speed, conventional hydrokinetic power generation application such as ocean current turbine is unable to operate. Thus, vortex induced vibration is put into consideration as the VIV based system have an ability to operate at low current condition.

III. RESULTS AND DISCUSSIONS

By using the equations discussed before, the optimum design for the VIV oscillator is determined.

*A. Optimum Size of Oscillator*

In order to estimate the required spring stiffness of cylinder oscillator, the frequency ratio is set to 1 in order to see its effect on the spring constant as well as the power output of the oscillator with varying diameter and length. The current speed  $U$  is also set at a constant flow which is 0.065 m/s.

TABLE I  
CALCULATION OF MASS OF APPLICATION AND ALTERATION OF SPRING CONSTANT FOR OSCILLATORS OF DIFFERENT SIZES

D [m]	L [m]	U m/s]	Re	Fs = Fn	k N/m]
0.30	2.40		19890	0.0429	17.3
0.20	1.60		13260	0.0644	11.5
0.10	0.80		6630	0.1287	5.8
0.08	0.64	0.065	5304	0.1609	4.6
0.06	0.48		3978	0.2145	3.4
0.04	0.32		2652	0.3218	2.3
0.02	0.16		1326	0.6435	1.2

TABLE II

CALCULATION OF POWER OUTPUT OF OSCILLATORS WITH DIFFERENT SIZES

<i>D</i> [m]	Lift Force [N]	<i>A</i> [m]	<i>Y</i> -Velocity [m/s]	<i>P</i> max [W]	<i>P</i> rms [W]
0.30	0.0605	0.0291	0.146	0.048	0.034
0.20	0.0269	0.0194	0.097	0.022	0.015
0.10	0.0067	0.0096	0.048	0.005	0.004
0.08	0.0043	0.0076	0.038	0.003	0.002
0.06	0.0024	0.0056	0.028	0.002	0.001
0.04	0.0011	0.0036	0.018	0.001	0.0005
0.02	0.0002	0.0013	0.007	0.0001	0.0001

Based on results calculated in Table II, the optimum size used for this project for the targeted offshore oil and gas platform is oscillator with diameter of 0.3 m and 2.4 m in length since it provides a much higher power output as compared to other sizes of studied oscillators. Although the larger the oscillator the higher its power output is, in terms of real life application, as the size of oscillator grows larger, the cost of building the application will increase tremendously especially when an array of the application is applied.

Current speed is set to as low as 0.065 m/s in order to confine the first study to the range of data obtained from Sabah Water Offshore Platform. The power output is low as well since the current calculation only consists of one single oscillator, instead of an array [10]. Based on Table II, oscillator with 0.3 m in diameter and 2.4 m in length provide the highest power RMS power output of 0.034 W with respect to the current speed of 0.065 m/s.

#### B. Best Spring Constant

Lock-in phenomenon is able to occur only when the frequency ratio is close or equal to 1. When such phenomenon occurs, the power output is much higher. In this section, varying spring constant will determine in which range of current speed lock-in phenomenon can occur, as well as comparing the power output when lock-in phenomenon happens. In this case, five different spring constants are tested and calculated as followed. The range of current speed studied is from 0.03 m/s to 0.12 m/s since this range is the current condition experiencing around Sabah Water Offshore Platform.

In order for a perfect lock-in condition to occur, Frequency ratio  $f^*$  must be close or equal to 1. To be more accurate, lock-in is considered to occur when the frequency ratio is 30% within the range, in this case, frequency ratio of less than 0.7 or above 1.3 are region where lock-in phenomenon fails to occur [6], [11]. Based on the results plotted in Table III, as the frequency ratio deviates away from 1, the power output is much lower compared to the frequency ratio close to one. Based on this study, application with spring constant 20 N/m is chosen as the best combination since lock-in phenomenon occurs most often for this spring.

TABLE III

CALCULATION OF POWER OUTPUT OF OSCILLATORS WITH DIFFERENT SPRING STIFFNESS

<i>D</i> [m]	<i>L</i> [m]	<i>U</i> [m/s]	<i>K</i> [N/m]	<i>F</i> s/ <i>F</i> n	<i>P</i> rms [W]
		0.03		0.428	0.000042
		0.04		0.572	0.00029
		0.05		0.714	0.00149
		0.06		0.857	0.00781
0.30	2.4	0.07	10	1.000	0.04664
		0.08		1.143	0.03714
		0.09		1.286	0.03765
		0.10		1.429	0.04508
		0.11		1.572	0.05687
		0.12		1.714	0.07284
		0.03		0.350	0.000032
		0.04		0.467	0.00020
		0.05		0.583	0.00091
		0.06		0.700	0.00352
0.30	2.4	0.07	15	0.817	0.01329
		0.08		0.933	0.06105
		0.09		1.050	0.12204
		0.10		1.167	0.09728
		0.11		1.283	0.10106
		0.12		1.400	0.11662
		0.03		0.304	0.000027
		0.04		0.406	0.00016
		0.05		0.507	0.00070
		0.06		0.609	0.00246
0.30	2.4	0.07	20	0.710	0.00782
		0.08		0.811	0.02468
		0.09		0.913	0.08910
		0.10		1.014	0.26738
		0.11		1.116	0.21231
		0.12		1.217	0.19847
		0.03		0.321	0.000029
		0.04		0.428	0.00018
		0.05		0.534	0.00077
		0.06		0.641	0.00277
0.30	2.4	0.07	18	0.748	0.00924
		0.08		0.855	0.03217
		0.09		0.962	0.13659
		0.10		1.069	0.18350
		0.11		1.176	0.15301
		0.12		1.283	0.15855
		0.03		0.272	0.000024
		0.04		0.363	0.00014
		0.05		0.454	0.00059
		0.06		0.544	0.00197
0.30	2.4	0.07	25	0.635	0.00584
		0.08		0.726	0.01627
		0.09		0.816	0.04569
		0.10		0.907	0.14379
		0.11		0.998	0.44172
		0.12		1.088	0.39370

#### C. Array of VIV Application

A single unit of VIV application is insufficient to generate power supply to accommodate the activities on offshore platforms. The results can be seen in section 4.2 as the power output for this particular VIV application is rather small

mainly due to the relatively small velocity of the current in the ocean near the proposed Sabah Water offshore Oil and Gas Platform. Thus, an array system should be constructed in order to generate sufficient power supply. The arrangement for the set of array based on VIV system power plant is modelled by assuming set distance between cylinders as shown in Fig. 4 which is recommended by VIVACE [6]. The array system can be calculated as the function of the cylinder diameter by assuming  $p$  and  $t$  are diameter linear functions using (19) and (20):

$$t(D) = 5 \times D \quad (19)$$

$$p(D) = 8 \times D \quad (20)$$

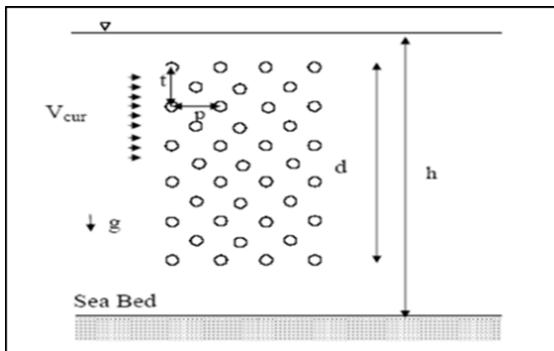


Fig. 4 Geometry and arrangement of cylinders in VIVACE Converter [6]

The cylinders attached onto the system as well as the volume of the array of system can be calculated using (21) and (22), where  $[a]$  is the number of cylinder parallel with the current flow,  $[b]$  is the number of cylinder with respect to height of array,  $[c]$  is the number of  $[a] \times [b]$  arrays into page and  $[L]$  is the length of cylinder.

$$N_{\text{cylinders}} = [a \times b \times c] + [(a - 1)(b - 1) \times c] \quad (21)$$

$$V(D) = [a \times t(D)] \times [b \times p(D)] \times [c \times L] \quad (22)$$

Then, the total power,  $P_{\text{total}}$  able to be generated as a system at whole can be determined by multiply the RMS power output generated by a single unit of cylinder with total number of cylinders in array system as shown in (23):

$$P_{\text{total}} = N_{\text{cylinders}} \times P_{\text{rms}} \quad (23)$$

The power density,  $PD(D)$  which is the function of cylinder diameter, can be generated by divided the maximum total power in array system with total volume of the array as shown in (24):

$$PD(D) = P_{\text{total}} / V(D) \quad (24)$$

The results of power output by the array of system are tabulated as followed. In this result, the value  $a$ ,  $b$ , and  $c$  are 4, 2 and 1 respectively. While the number of cylinder used is 39

for this array of system.  $D$  is the diameter of the cylindrical oscillator, while  $L$  is the length of the oscillator into the page. The power output and the power density of the array are calculated and tabulated in Table IV.

TABLE IV  
POWER OUTPUT OF SINGLE ARRAY OF VIV APPLICATION

$U[\text{m}]$	$p(D)$	$t(D)$	$N_{\text{cylinder}}$	$P_{\text{total}}[\text{W}]$
0.03				0.0011
0.04				0.0064
0.05				0.0273
0.06				0.0960
0.07				0.3049
0.08	0.6	0.3	39	0.9625
0.09				3.4747
0.10				10.4276
0.11				8.2801
0.12				7.7405

Based on Table IV, the maximum power output of a single array at current speed of 0.12 m/s hit as high as 7.74 W. However in this region, based on Table III for spring constant 20 N/m, lock-in phenomenon did not occur completely due to the fact that the frequency ratio is off by about 20% from the ideal lock-in. At current speed of 0.1 m/s, since the frequency ratio is having the value of 1.01, lock-in phenomenon occurs completely. It showed that as the shedding frequency becomes close to natural frequency that gives the frequency ratio equal to 1, the amplitude and velocity of cylinder will increase and resulting in higher power output [12]. In this case, the power output of cylinder on current flow 0.10 m/s is highest although the current flow is lower than 0.12 m/s, which gives out the rated power output as high as 10.4 W.

#### IV. CONCLUSION

Vortex induced vibration application in generating energy is a viable solution as an alternative energy for offshore application. VIV have an ability to provide energy in low speed current region where the conventional hydrokinetic application is unable to operate. Although the power output might be relatively low, this technology is considered new and thus improvement in various segments can be further improved from time to time. With current speed as low as 0.1 m/s, the VIV application designed is able to provide a rated power output as high as 10.4 W with just a single array. When a farm of such application is constructed, the power supply can be increased and able to support various industries ranges from offshore platforms to even ground activities. VIV also has the potential to be integrated and applied on the offshore platform with the other renewable energy technologies such as solar, wind and tidal.

#### REFERENCES

- [1] J. Rosebro, Fossil-Fuel Platform Runs on Renewable Energy, 2006. [http://www.greencarcongress.com/2006/04/fossilfuel\\_plat.html](http://www.greencarcongress.com/2006/04/fossilfuel_plat.html)
- [2] E. Goffman, Why Not the Sun? Advantages of and Problems with Solar Energy, *Journal of ProQuest Discovery Guides*, 2008.

- [3] R. C. Sharma, and N. Sharma, Energy from Ocean and Scope of its Utilization in India, *Journal of Environmental Engineering and Management*, Vol. 4, pp.397-404, 2013.
- [4] Commission of the European Commission, DGXII, Wave Energy Project Result: The exploitation of Tidal Marine Currents, *Report EUR16683EN*, ISSN 1018-5593, 1996.
- [5] T. Ball, K. Thomas, S. Shubham, W. Ethan, Maximizing Vortex Induce Vibrations Through Geometry Variation, *Major Qualifying Project: 1-89*. 2012.
- [6] M. M. Bernitsas, K. Raghavan, Y. Ben-Simon, and E. M. Garcia, VIVACE (Vortex Induced Vibration Aquatic Clean Energy): A New Concept in Generation of Clean and Renewable Energy from Fluid Flow, *Journal of Offshore Mechanics and Arctic Engineering*, 2006.
- [7] A. Techet, Vortex Induced Vibration. MIT OpenCourseWare, Massachusetts Institute of Technology, United States, 2005.
- [8] P. Bassani, E. Gariboldi and A. Tuissi, Calorimetric Analysis of AM60 Magnesium Alloy. *Journal of Thermal Analysis and Calorimetry*, Vol. 80, pp. 739-747, 2005.
- [9] A. Hall-Stinson, C. Lehrman, and E. Tripp, *Energy Generation from Vortex Induced Vibration*, Thesis (B.S.), Worcester Polytechnic Institute, United States, 2011.
- [10] M.A. Zahari and S.S. Dol, Application of Vortex Induced Vibration Energy Generation Technologies to the Offshore Oil and Gas Platform: The Preliminary Study, *International Journal of Mechanical, Aerospace, Industrial and Mechatronics Engineering*, 8(7), pp. 1313-1316, 2014.
- [11] M.A. Zahari, S.S Dol, Alternative Energy using Vortex-induced Vibration from Turbulent Flows: Theoretical and Analytical Analysis, *5th Brunei International Conference on Engineering and Technology, IEEE Xplore Digital Library*, 2014.
- [12] M.A. Zahari, S.S Dol, Effects of Different Sizes of Cylinder Diameter on Vortex-Induced-Vibration for Energy Generation, *Journal of Applied Sciences*, 15(5), pp. 783-791, 2015.